AMERICAN SOCIETY FOR MICROBIOLOGY | Journal of Virology®

PATHOGENESIS AND IMMUNITY

Sequence Evaluation and Comparative Analysis of Novel Assays for Intact Proviral HIV-1 DNA

Christian Gaebler,[a] Shane D. Falcinelli,[b,c] Elina Stoffel,[a] Jenna Read,[b] Ross Murtagh,[b] Thiago Y. Oliveira,[a] Victor Ramos,[a] Julio C. C. Lorenzi,[a] Jennifer Kirchherr,[b] Katherine S. James,[b] Brigitte Allard,[b] Caroline Baker,[b] JoAnn D. Kuruc,[b,d] Marina Caskey,[a] Nancie M. Archin,[b,d] Robert F. Siliciano,[e,f] David M. Margolis,[b,c,d] Michel C. Nussenzweig[a,g]

[a]Laboratory of Molecular Immunology, The Rockefeller University, New York, New York, USA
[b]UNC HIV Cure Center, University of North Carolina, Chapel Hill, North Carolina, USA
[c]Department of Microbiology and Immunology, University of North Carolina, Chapel Hill, North Carolina, USA
[d]Department of Medicine, University of North Carolina, Chapel Hill, North Carolina, USA
[e]Department of Medicine, Johns Hopkins University School of Medicine, Baltimore, Maryland, USA
[f]Howard Hughes Medical Institute, Baltimore, Maryland, USA
[g]Howard Hughes Medical Institute, The Rockefeller University, New York, New York, USA

Christian Gaebler and Shane D. Falcinelli contributed equally to this work. Author order was determined on the basis of the contribution to development and analysis of the work.

ABSTRACT The HIV proviral reservoir is the major barrier to cure. The predominantly replication-defective proviral landscape makes the measurement of virus that is likely to cause rebound upon antiretroviral therapy (ART)-cessation challenging. To address this issue, novel assays to measure intact HIV proviruses have been developed. The intact proviral DNA assay (IPDA) is a high-throughput assay that uses two probes to exclude the majority of defective proviruses and determine the frequency of intact proviruses, albeit without sequence confirmation. Quadruplex PCR with four probes (Q4PCR) is a lower-throughput assay that uses limiting dilution long-distance PCR amplification followed by quantitative PCR (qPCR) and near-full-length genome sequencing (nFGS) to estimate the frequency of sequence-confirmed intact proviruses and provide insight into their clonal composition. To explore the advantages and limitations of these assays, we compared IPDA and Q4PCR measurements from 39 ART-suppressed people living with HIV. We found that IPDA and Q4PCR measurements correlated with one another, but frequencies of intact proviral DNA differed by approximately 19-fold. This difference may be in part due to inefficiencies in long-distance PCR amplification of proviruses in Q4PCR, leading to underestimates of intact proviral frequencies. In addition, nFGS analysis within Q4PCR explained that some of this difference is explained by proviruses that are classified as intact by IPDA but carry defects elsewhere in the genome. Taken together, this head-to-head comparison of novel intact proviral DNA assays provides important context for their interpretation in studies to deplete the HIV reservoir and shows that together the assays bracket true reservoir size.

IMPORTANCE The intact proviral DNA assay (IPDA) and quadruplex PCR (Q4PCR) represent major advances in accurately quantifying and characterizing the replication-competent HIV reservoir. This study compares the two novel approaches for measuring intact HIV proviral DNA in samples from 39 antiretroviral therapy (ART)-suppressed people living with HIV, thereby informing ongoing efforts to deplete the HIV reservoir in cure-related trials.

KEYWORDS HIV cure, HIV latent reservoir, human immunodeficiency virus

Latent replication-competent HIV proviruses are a formidable barrier to HIV cure, but there is little consensus on how to best measure this reservoir (1). Available assays for the reservoir include measurements of HIV DNA, inducible HIV RNA/protein, and

Citation Gaebler C, Falcinelli SD, Stoffel E, Read J, Murtagh R, Oliveira TY, Ramos V, Lorenzi JCC, Kirchherr J, James KS, Allard B, Baker C, Kuruc JD, Caskey M, Archin NM, Siliciano RF, Margolis DM, Nussenzweig MC. 2021. Sequence evaluation and comparative analysis of novel assays for intact proviral HIV-1 DNA. J Virol 95:e01986-20. https://doi.org/10.1128/JVI.01986-20.

Editor Guido Silvestri, Emory University

Address correspondence to David M. Margolis, dmargo@med.unc.edu, or Michel C. Nussenzweig, nussen@rockefeller.edu.

Received 7 October 2020
Accepted 7 December 2020
Accepted manuscript posted online 23 December 2020
Published 24 February 2021

quantitative viral outgrowth assays (2). Comparisons of different reservoir measurements provide useful insights into the nature of the HIV reservoir. For example, comparison of reservoir measurements revealed a greater than 2-log discrepancy between the frequency of integrated proviruses measured by DNA PCR and replication-competent proviruses measured by viral outgrowth (3). This discrepancy is largely explained by the disproportionate frequency of defective proviral DNA and variable inducible outgrowth of intact proviruses (4, 5). Thus, single-probe HIV DNA PCR-based assays are limited in specificity for intact HIV genomes because a large fraction of the proviruses that they detect are defective.

Although quantitative viral outgrowth assays are specific for intact HIV genomes, they are labor-intensive, and the results vary over time by as much as a factor of 6 (6). Furthermore, they underestimate the frequency of intact HIV genomes because not all proviruses are equally inducible *in vitro* (5, 7). As such, many intact proviruses are not detected in outgrowth assays. To improve on the specificity of PCR-based assays for detection of intact proviruses, novel methods have been developed that combine probes that target relatively conserved regions of the genome (intact proviral DNA assay [IPDA]) (8) in addition to limiting dilution near-full-genome proviral sequencing (a component of Q4PCR) (9).

The IPDA utilizes digital droplet PCR (ddPCR) to measure proviruses with probes targeting conserved regions in the packaging signal (PS) and envelope (*env*) that when amplified together in the same provirus, exclude the majority of defective proviruses. Input cells are directly measured by a simultaneous ddPCR reaction, enabling the IPDA to report the total frequency of intact and defective proviruses per million input cells. The Q4PCR assay employs long distance PCR at limiting dilution to amplify proviruses, followed by interrogation with four quantitative PCR (qPCR) probes for PS, *env*, *pol*, and *gag* in a multiplex reaction to detect amplified HIV-1 genomes. Cell inputs are estimated by quantification of input DNA, and the frequency of intact proviruses is reported after sequence verification by near-full-length genome sequencing (nFGS). Because the Q4PCR employs limiting dilution near-full-length proviral amplification, these nFGS results can be used to provide insight into the clonal composition of intact proviruses.

Here, we compare quantitative viral outgrowth assays, Q4PCR, IPDA, and total HIV *gag* DNA measurements on samples from 39 antiretroviral therapy (ART)-suppressed people living with HIV (PLWH) to explore the advantages and limitations of these assays.

RESULTS

Quantitative comparison. Leukapheresis or whole blood samples were obtained from PLWH, stably suppressed (<50 copies of HIV-1 RNA/ml) on ART under protocols approved by the University of North Carolina (UNC) or Rockefeller University biomedical institutional review boards. The majority of study participants were treated during chronic infection and had been on ART for a median of 8.4 years (see Table S1 in the supplemental material). For all 39 participants, Q4PCR and IPDA were performed on DNA extracted from total CD4 (tCD4) T cells from these two cohorts. Total HIV *gag* DNA was measured in tCD4 T cells using an assay designed to capture group M HIV-1 proviral DNA (10). Finally, we performed quantitative and qualitative viral outgrowth assay (Q^2VOA) ($n = 11$, Rockefeller cohort, tCD4 cells) or quantitative viral outgrowth assay (QVOA) ($n = 13$, UNC cohort, resting CD4 T cells) to measure inducible replication-competent HIV.

As expected, the sum of the IPDA-derived intact, 3′-defective, and 5′-defective proviral frequencies (IPDA total) yielded the highest proviral frequency estimates (median, 652 copies/million CD4 T cells), and quantitative viral outgrowth assays yielded the lowest across both cohorts (median, 0.60 infectious units/million CD4 T cells) (Fig. 1A). Median proviral frequency using a single-probe long terminal repeat (LTR)-*gag* assay (*gag* DNA) was 387 copies/million CD4 T cells. As expected, total HIV DNA frequency

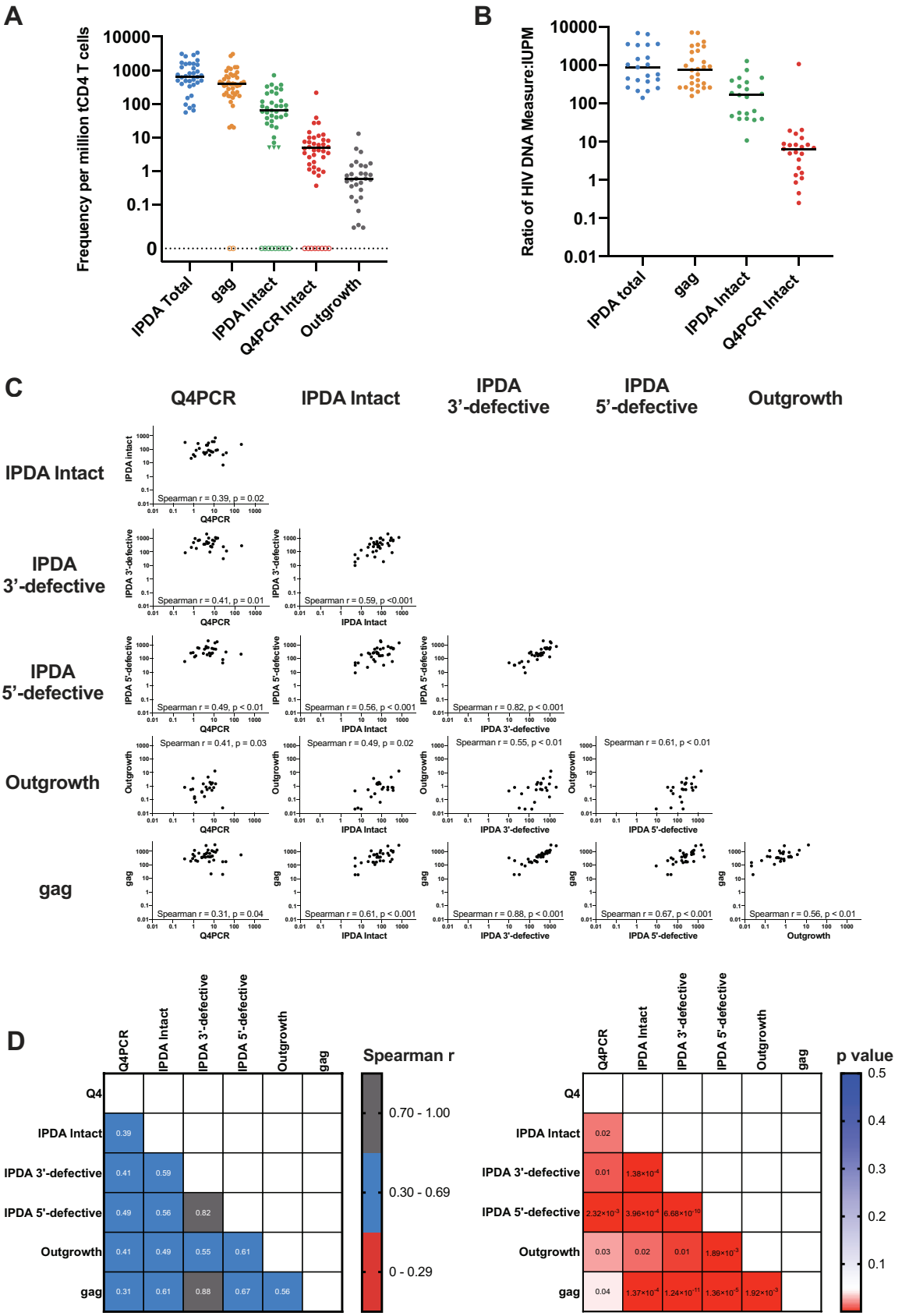

FIG 1 Quantitative Comparison of Reservoir Measurements. (A) Frequency per million total CD4 T cells for total HIV *gag*, intact provirus (IPDA), intact provirus (Q4PCR), and replication-competent outgrowth viruses. Triangles indicate left-censored measurements

(Continued on next page)

estimates (IPDA total DNA and *gag* DNA) were strongly correlated (Spearman $r = 0.86$, $P = 0.001$).

The frequency of intact HIV genomes detected by IPDA and Q4PCR were intermediate between *gag* DNA and viral outgrowth, consistent with previous studies with these assays and with previous estimates based on limiting dilution proviral nFGS (4, 8, 9, 11). For IPDA, proviruses were considered intact if they were positive for both PS and *env* probes. For Q4PCR, proviruses were considered intact if they were sequence verified. The median intact proviral frequency per million CD4 T cells was 65 for IPDA and 5 for Q4PCR (Fig. 1A). IPDA measurements were a median of 19 (interquartile range 7 to 48)-fold higher than Q4PCR measurements. Compared to outgrowth assays, the median ratio of gag DNA (779), intact sequences by IPDA (169), or Q4PCR (7) was greater than one (Fig. 1B).

To further understand the relationship between the assays, we calculated the Spearman correlation between *gag*, IPDA intact, IPDA 3′-defective, IPDA 5′-defective, infectious units per million (IUPM), and Q4PCR intact (Fig. 1C and D). IPDA and Q4PCR measures of intact DNA showed similar correlations with quantitative viral outgrowth measures (Spearman $r = 0.49$ and 0.41, respectively) and with each other (Spearman $r = 0.39$). IPDA and Q4PCR both moderately correlated with *gag* DNA ($r = 0.61$ and $r = 0.31$, respectively), in agreement with a previous report comparing IPDA and *gag* measurements (12). The 5′-defective and 3′-defective proviral frequencies measured using the IPDA also moderately correlated with quantitative viral outgrowth, IPDA intact, and Q4PCR proviral frequencies (Fig. 1C and D).

IPDA and Q4PCR proviral amplification. We observed amplification signal failure of either the PS or *env* IPDA primer/probe sets for 7 (18%) of the 39 participants (0 of 12 from the UNC cohort, and 7 of 27 from the Rockefeller cohort). In addition, another small subset of samples (4 of 39; 10.3%) showed reduced fluorescent signal intensities in the PS or *env* IPDA primer/probe set, thereby complicating the unambiguous identification of a distinct double positive droplet population. With Q4PCR, we were able to identify sequences that were positive for 2 or more probes in 37 of the 39 individuals (9). However, we did not detect intact sequences from 8 of the 39 participants (20.5%).

We determined viral genotypes using the Q4PCR sequencing data. Overall, we identified 3 participants (one from the UNC cohort, two from the Rockefeller cohort) with non-subtype B viral infection (clades A1 and G). For 2 of the 3 non-subtype B-infected individuals, we observed IPDA amplification failures in the *env* IPDA probe, reflecting the fact that the initial version of the IPDA was designed based on clade B sequence data (8). In contrast, using Q4PCR, we retrieved intact proviral sequences from 2 of the 3 individuals with non-subtype B viruses. The utilization of 4 instead of 2 probes appears to render Q4PCR less sensitive to subtype variability. For example, *env* amplification failed for participant 5112 in both assays, but several intact proviral genomes scored positive for the PS, *pol*, and *gag* probe by Q4PCR (Fig. 2C).

For the fraction of participants harboring clade-B viruses, the frequency of IPDA amplification signal failure was 14.7%, which is similar to but slightly higher than that reported by others in larger cohorts (11) (Fig. 2A and Table S2).

FIG 1 Legend (Continued)
for the IPDA (detectable defective proviruses but no PS+*env*+ proviruses; see Materials and Methods). Assay data from participants with an amplification failure (7/39 for IPDA, 2/39 for *gag*) or no recovery of intact proviral sequences for Q4PCR (8/39) are represented as hollow symbols and were excluded from the analysis, but other assay data for those participants were included if available. (B) Frequency ratio with viral outgrowth measures (IUPM) as the denominator for total HIV *gag*, intact provirus (IPDA), and intact provirus (Q4PCR). Data points that were left-censored, had an IPDA amplification failure, or had no recovered Q4PCR intact proviral sequences were excluded for this analysis. (C) Scatterplots showing correlations of reservoir measurements, including Spearman *r* and unadjusted *P* values. Left-censored measurements were included as follows: for Q4PCR, when no intact proviruses were recovered, a value of 0 was used, and for IPDA, a left-censor of 5 copies/million CD4 T cells was used as described in Materials and Methods. Data points were excluded when an IPDA amplification failure was present. (D) Spearman correlation and *P* value matrices comparing all available reservoir measurements. *P* values are unadjusted. Left-censored measurements were included as follows: for Q4PCR, when no intact proviruses were recovered, a value of 0 was used, and for IPDA, a left-censor of 5 copies/million CD4 T cells was used as described in Materials and Methods. Data points were excluded when an IPDA amplification failure was present.

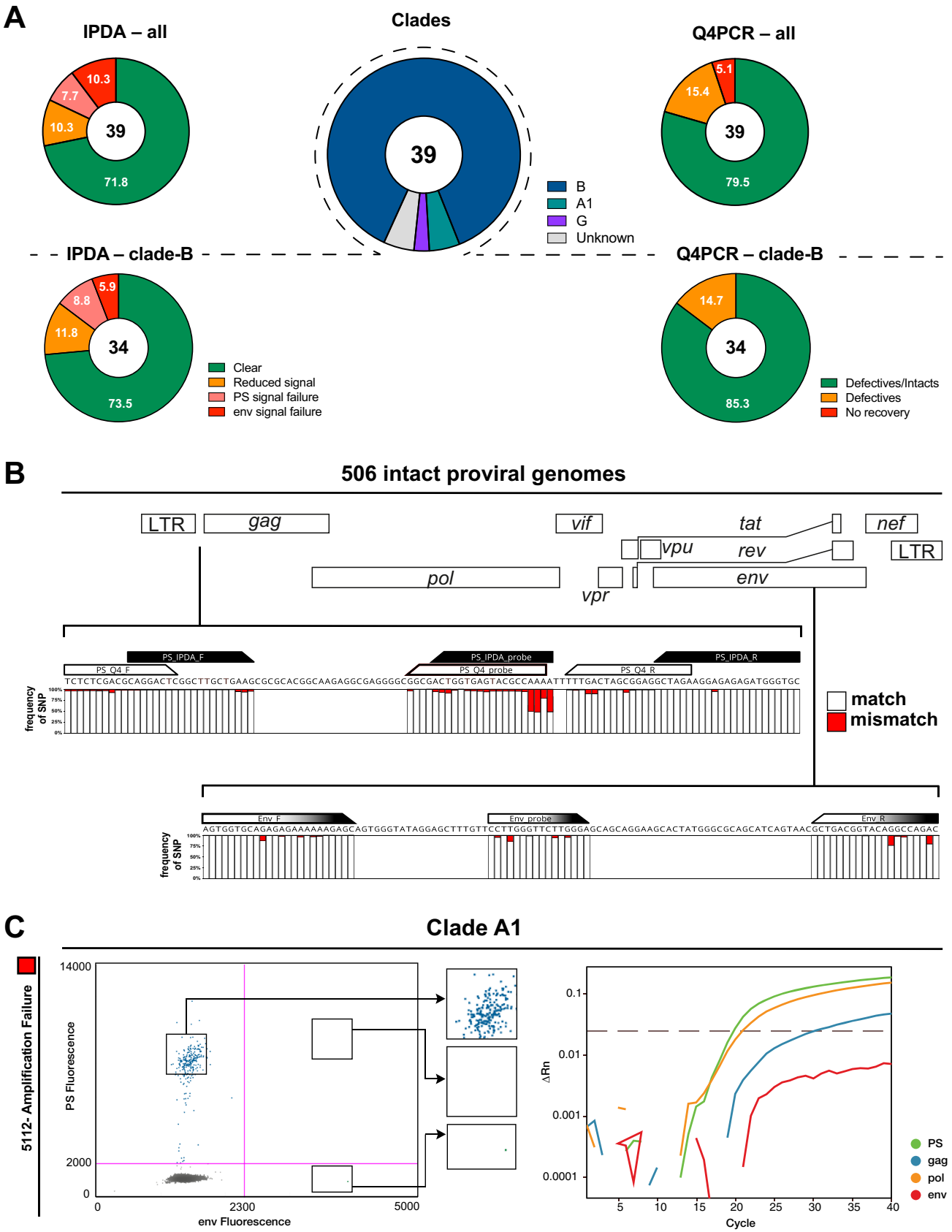

FIG 2 (A) IPDA and Q4PCR signal summary. Pie charts on the left depict the fraction of participants that showed an IPDA amplification failure for PS (light red slice) or *env* (dark red slice), reduced signal intensities/droplet separation (orange slice) or clear results (green slice) for all viral genotypes

(Continued on next page)

PS and *env* sequence conservation among intact proviruses. Overall, we found 506 intact and 4,211 defective proviral sequences by Q4PCR (Table 1). The IPDA and Q4PCR utilize overlapping primer/probe sets in PS and identical primer/probe in *env* (9). To determine the level of sequence conservation in the primer/probe binding regions in our study participants at a single nucleotide resolution we aligned all 506 intact proviral genomes from Q4PCR nFGS.

As expected, the binding regions of the IPDA/Q4PCR PS and *env* primer/probe sets showed high levels of conservation among the intact proviral genomes (8, 9). Nevertheless, single nucleotide polymorphisms (SNP) could be detected to various degrees in all primers and probes of both PS and *env*. While the occurrence of common SNPs in the 5′ region of primers/probes (e.g., up to 50% in the 5′ PS probe region) are expected to have little impact on signal quality, a mismatch in the very 3′ end of the primers/probes (e.g., 6% SNP frequency in the IPDA PS forward primer 3′ end) can impact signal detection considerably (13, 14) (Fig. 2B).

PS and *env* sequence polymorphism analysis. To examine the importance of HIV diversity on an individual level, we next used the Q4PCR sequence information to study polymorphisms and associated signal patterns for individual participants.

In most cases, the quality of IPDA and Q4PCR signal could be explained by the absence or presence of sequence polymorphisms in the primer/probe binding regions of proviral genomes. For example, intact proviruses from participant UNC-434 showed complete conservation in the primer/probe binding regions, resulting in clear and distinct IPDA and Q4PCR PS and *env* signals (Fig. 3A). In contrast, the amplification failure of the IPDA PS signal in participant 9243 could be explained by a two-nucleotide mismatch at the 3′ end of the PS IPDA forward primer (Fig. 3B). In addition, single nucleotide polymorphisms in the *env* primer/probe region of intact proviruses from participant 5101 (Fig. 3C) resulted in signal reduction rather than the complete amplification failure for the IPDA. While such a decrease in droplet separation complicates the clear identification of PS+*env*-positive proviruses by IPDA, PCR annealing temperature decreases were shown to improve droplet resolution (Fig. 4A). Proviral signal patterns (droplet amplitude or qPCR amplification curves) were found to be stable over time in all six individuals that were assayed at more than one time point, thereby demonstrating the consistent impact of sequence polymorphisms on signal patterns. However, occasional discordant results between qPCR amplification and sequencing results require further study.

PS and *env* intact proviral genome prediction. Intact proviral DNA detection assays face the challenges of both detecting viral sequences and correctly characterizing them as intact or defective. Using nFGS data, Bruner and colleagues reported that the IPDA PS and *env* primer/probe sets exclude 97% of proviruses with defects detectable by nFGS and that approximately 70% of proviruses classified as intact by IPDA lack defects detectable by nFGS (8).

We used Q4PCR sequencing data to assess the fraction of true intact sequences out of all samples that were amplified by the Q4PCR PS and *env* primer/probe set combination. We considered a total of 4,717 proviruses collected from all wells positive for 2 or more of the quadruplex qPCRs of the Q4PCR. Notably, proviral sequence was not collected from wells positive for only one qPCR in the Q4PCR, which likely contain defective proviruses (9). A total of 29 PS+*env*-positive sequences with a threshold cycle

FIG 2 Legend (Continued)
(upper panel) or only clade-B viruses (lower panel). Similarly, pie charts on the right depict the fraction of participants that yielded no sequence information (red slice), only defective proviral sequences (orange slice), or both defective and intact sequences (green slice) for all viral genotypes (upper panel) or only clade-B viruses (lower panel). The pie chart in the center shows the distribution of viral genotypes among the 39 participants (clade B [blue], A1 [green], G [purple], or unknown [gray]). (B) Sequence conservation in IPDA and Q4PCR PS+*env* primer/probe binding regions among 506 intact proviral genomes. Stacked bar graphs show sequence identity obtained by aligning all intact proviral sequences with the PS primer/probe set (IPDA PS primer/probe set in black, Q4PCR PS primer/probe set in white) and *env* primer/probe set (identical for IPDA and Q4PCR, depicted in black and white). White or red bars represent the frequencies of single-nucleotide polymorphisms (SNPs) that match (white) or mismatch (red) the primer/probe in a specific nucleotide. (C) Non-clade B signal quality. Example of an amplification failure of the *env* signal in IPDA for participant 5112. The corresponding Q4PCR signal of an intact proviral genome also shows an *env* signal failure but at the same time a clear signal for the PS and *pol* probe demonstrating less susceptibility to non-clade B viral genotypes for Q4PCR.

TABLE 1 The number of sequences obtained by Q4PCR for each of the 39 participants

Participant ID	Total no. sequenced	No. of intact sequences	No. of defective sequences
5101	156	4	152
5104	158	124	34
5105	120	3	117
5106	20	14	6
5108	76	19	57
5111	101	8	93
5112	74	6	68
5114	60	4	56
5115	17	0	17
5203	29	15	14
603	461	8	453
605	90	6	84
9242_wk-2	318	38	280
9242_wk12	303	31	272
9243_wk-2	195	8	187
9243_wk12	93	3	90
9244_wk-2	155	10	145
9244_wk12	127	6	121
9246	32	1	31
9247	49	26	23
9241	134	6	128
9252_wk-2	213	19	194
9252_wk12	241	7	234
9254	98	42	56
9255_wk-2	306	20	286
9255_wk12	261	24	237
B207	57	13	44
TSC124	7	0	7
TSC125	20	1	19
TSC127	136	9	127
TSC128	41	4	37
TSC131	1	0	1
UNC308	122	2	120
UNC336	0	0	0
UNC346	155	8	147
UNC367	143	5	138
UNC397	0	0	0
UNC404	35	1	34
UNC-406,425_wk48	0	0	0
UNC-406,425_wk96	5	0	5
UNC412	15	1	14
UNC432	43	1	42
UNC434	46	9	37
UNC437	3	0	3
UNC458	1	0	1

(C_T) of >38 were excluded. Out of the remaining 4,688 proviral genomes, only 625, or 13.3%, scored positive with PS+*env* (C_T, <38 for both amplicons). Out of 4,139 defective proviruses positive for 2 or more of the quadruplex qPCRs in Q4PCR, only 305 (7.4%) were found to be positive for the combination of PS+*env*, thereby demonstrating the exceptional specificity of this particular probe combination to exclude defective proviruses (9). At the same time, the Q4PCR PS+*env* combination failed to detect 175 (35.3%) out of 475 intact proviruses. The majority of the 175 PS+*env*-negative intact genomes were recovered from individuals with amplification signal failures of either the PS or *env* primer/probe set, and only the utilization of two additional probes (*gag* and *pol*) enabled the detection and intact sequence verification by Q4PCR (Fig. 4A). Signal failure was generally consistent between Q4PCR and IPDA, except where there were signal-eliminating polymorphisms in the Q4PCR but not

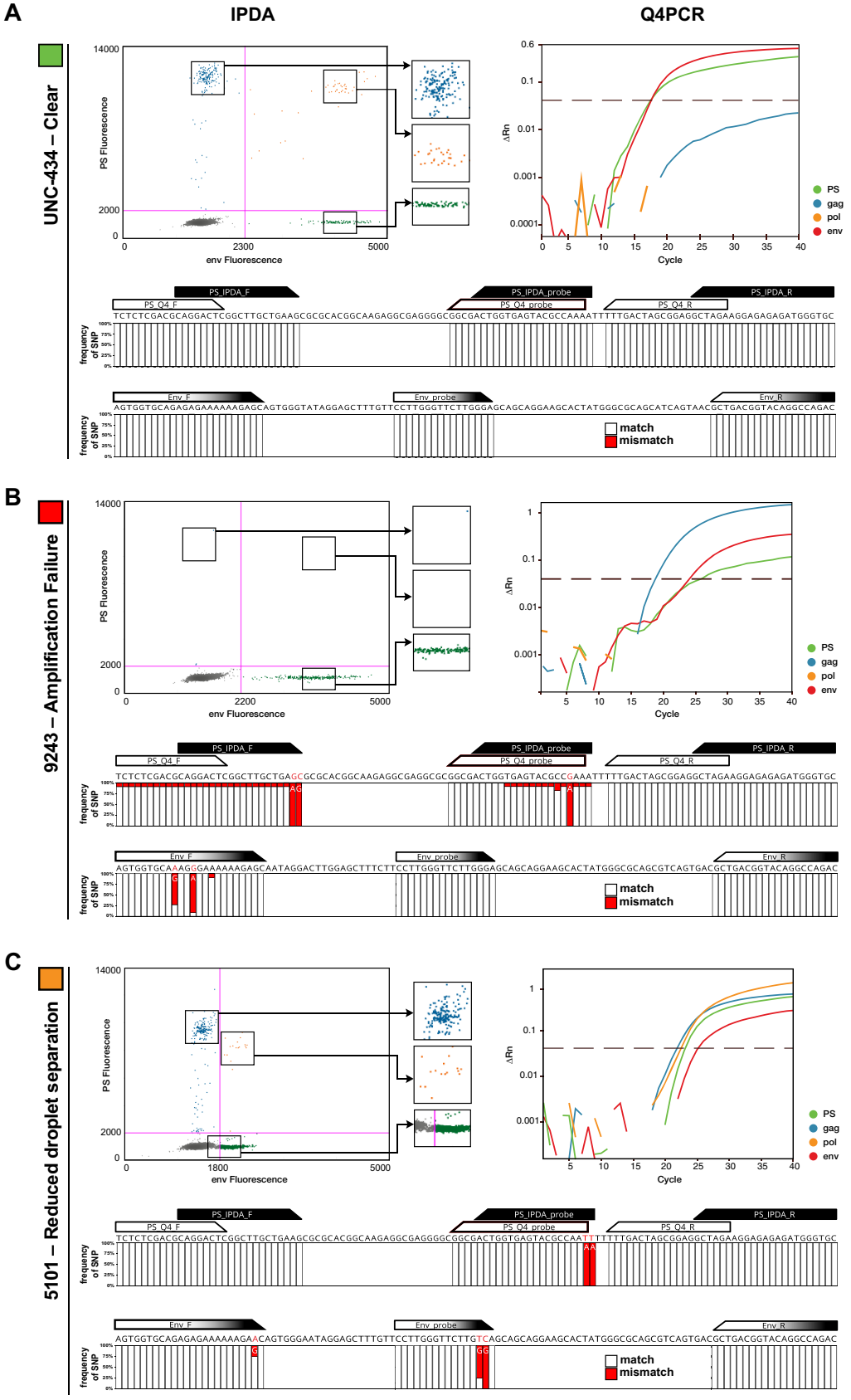

FIG 3 PS and *env* sequence polymorphism analysis. (A) Example of a clear droplet distribution for the PS (blue), *env* (green), and PS+*env*-positive (orange) droplets by IPDA and the corresponding Q4PCR signal (PS, green; *gag*, blue;

(Continued on next page)

the IPDA PS primer/probe set or vice-versa (Fig. 3B). Importantly, amplicon signal failure in the IPDA is readily apparent, and intact provirus values are not reported in these cases (11).

Of all 625 PS+*env*-positive samples, 320, or only 51.2%, were actually identified as intact proviral genomes on a sequence level. To assess the percentage of PS+*env*-positive samples that were truly intact by nFGS on an individual participant basis, we analyzed individuals with at least 5 PS+*env*-positive sequences (Table 2). Importantly, and in line with our previous study, the percentage of PS+*env*-positive proviruses that were truly intact by nFGS appeared to vary between individuals (Fig. 4B) (9). PS+*env*-positive proviruses are scored as intact by IPDA. However, we found that the frequencies of PS+*env*-positive proviruses detected by Q4PCR were a median of 6-fold (interquartile range 2 to 17) lower than IPDA measurements (Table S2). Further, after sequence verification, Q4PCR values for intact viruses were substantially lower (by a median of 19-fold) than IPDA. Both of these results suggest that limitations of long-distance PCR amplification in Q4PCR as well as the IPDA misidentification of some PS and *env* amplifiable sequences as intact contribute to differences in the quantification of the intact proviral reservoir (Table 3).

DISCUSSION

We compared the results of some of the available HIV-1 reservoir assays, including Q4PCR and IPDA, because quantitation and characterization of the HIV reservoir informs efforts to develop an HIV cure (1). The great majority of integrated HIV proviral DNA is defective. Outgrowth assays quantitate the replication-competent reservoir, but they are labor-intensive and not scalable to large clinical studies. In addition, they do not capture all replication-competent viruses. The IPDA and Q4PCR were designed to address some of these issues. The IPDA utilizes ddPCR to measure proviruses that are PS+*env*-positive, which together exclude the great majority of defective proviruses with defects detectable by nFGS. This assay enables much more specific quantification of intact proviral DNA than single-probe assays. However, the PS and *env* probe combination is not entirely predictive of a fully intact provirus (8, 9). Q4PCR improves the sensitivity and specificity of PCR-based assays for intact HIV DNA using a combination of qPCR and sequencing (9). The Q4PCR assay employs four different qPCR probes for PS, *env*, *pol*, and *gag* in a multiplex reaction to detect the HIV-1 genome in limiting dilution samples. Samples positive for 2 or more probes are subjected to near-full-length sequencing to verify the intactness of the provirus, enabling a very high specificity for intact proviruses. However, this assay is not scalable for a large number of samples precisely because it requires limiting dilution PCR and full-length proviral DNA sequencing.

Our results show that Q4PCR and IPDA are positively correlated but differ in that IPDA identifies a higher number of intact proviruses than Q4PCR. Several possibilities, which are not mutually exclusive, may explain why intact proviral frequency estimates from Q4PCR were a median of 19-fold lower than those from IPDA (9).

First, limitations of long-distance PCR amplification in Q4PCR may have a positive bias toward amplification and subsequent quantification of defective proviruses due

FIG 3 Legend (Continued)
pol, yellow; *env*, red) for participant UNC-434. Stacked bar graphs depict sequence alignment of all intact proviral sequences from participant UNC-434 with the PS primer/probe set (IPDA PS primer/probe set in black, Q4PCR PS primer/probe set in white) and *env* primer/probe set (identical for IPDA and Q4PCR, depicted in black and white). White or red bars represent the frequencies of single-nucleotide polymorphisms (SNPs) that match (white) or mismatch (red) the primer/probe in a specific nucleotide. (B) Example of an amplification failure of the PS signal by IPDA for participant 9243. The corresponding Q4PCR signal and intact proviral genome alignment reveal an explanatory two-nucleotide mismatch in the IPDA PS forward primer 3′ end across all intact proviral genomes from participant 9243. (C) Example of a reduced droplet distribution in the IPDA *env* signal, thereby complicating the clear separation of the PS+*env*-positive droplets from the negative population for participant 5101. The corresponding Q4PCR signal shows a reduced signal intensity for the *env* signal as well. The intact proviral genome alignment depicts an explanatory two-nucleotide mismatch in the IPDA/Q4PCR probe 3′ end.

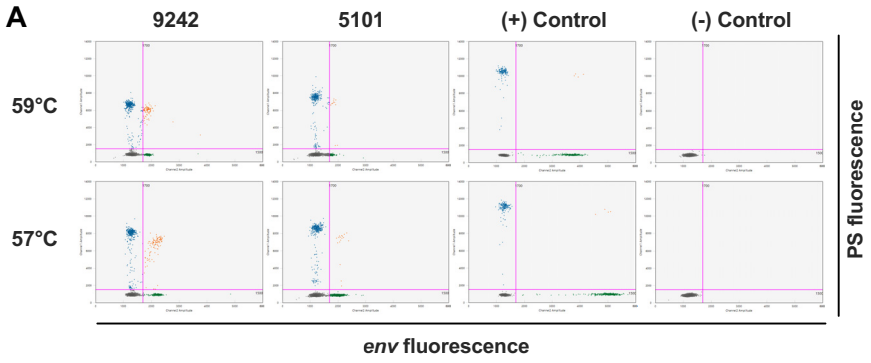

B

		nFGS		
		Intact	Defective	Total
Q4PCR	PS+*env* pos.	320	305	625 (13.3%)
	PS+*env* neg.	175	3888	4063 (86.7%)
	Total	495 (10.6%)	4193 (89.4%)	4688 (100%)

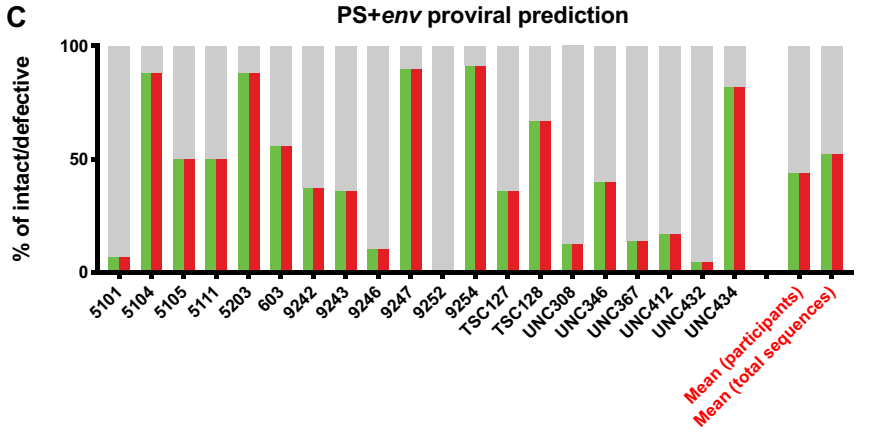

FIG 4 Q4PCR PS and *env* intact proviral genome prediction. (A) Improved droplet separation for the IPDA with 57°C versus 59°C annealing temperature. Droplet amplitude improved, especially for the *env*/VIC amplicon, with a PCR annealing temperature of 57°C versus 59°C without compromising the ability of the *env* hypermutated probe to discriminate hypermutated sequences (data not shown). (B) The 2-by-2 table shows the number of PS+*env*-positive and PS+*env*-negative samples by Q4PCR and the corresponding classification as intact or defective proviral genomes based on near-full-length sequencing results. To improve signal-to-background, we excluded 29 sequences with C_T values greater than 38 for either the PS or *env* primer/probe set. (C) PS+*env* proviral sequence prediction. Q4PCR sequencing data were used to assess the fraction of true intact sequences out of all samples that were amplified by the Q4PCR PS and *env* primer/probe set combination on an individual participant basis. The graph shows the percentage of proviruses detected by the Q4PCR PS+*env* primer/probe combination that were truly intact by nFGS for 20 individuals with at least 5 PS+*env*-positive sequences. The predictive value for intact proviruses is colored in green (PS) and red (*env*). The defective fraction is shown in gray. The right two bar graphs depict the mean percentage of PS+*env*-positive samples that were truly intact by nFGS in a pooled analysis of all sequences (first bar graph to the right) or averaged across all 20 participants (second bar graph to the right), respectively.

to their shorter length from large deletions (15, 16). Inefficient amplification may account for the high degree of variation between the number of estimated intact genomes measured by different nFGS assays (4, 5, 9, 17–21), and it may explain why intact proviruses are not detected by Q4PCR in approximately 20% of infected

TABLE 2 The number and classification (intact versus defective) of PS+*env*-positive samples for all participants with at least 5 PS+*env*-positive samples

Participant ID	Total no. of sequences	No. of intact sequences	No. of defective sequences	Intact sequences (%)
5101	58	4	54	6.9
5104	140	123	17	87.9
5105	6	3	3	50.0
5111	8	4	4	50.0
5203	17	15	2	88.2
603	9	5	4	55.6
9242	137	51	86	37.2
9243	25	9	16	36.0
9246	10	1	9	10.0
9247	29	26	3	89.7
9252	11	0	11	0.0
9254	46	42	4	91.3
TSC127	14	5	9	35.7
TSC128	6	4	2	66.7
UNC308	8	1	7	12.5
UNC346	20	8	12	40.0
UNC367	22	3	19	13.6
UNC412	6	1	5	16.7
UNC432	22	1	21	4.5
UNC434	11	9	2	81.8

individuals. In addition, even after correction for defects missed by the IPDA amplicons, intact provirus values measured by IPDA are substantially higher that those obtained by Q4PCR (Table S2).

A second factor that may contribute to higher intact proviral measurements in the IPDA versus Q4PCR is cell normalization methods. The IPDA normalizes proviral frequencies to cell input by quantifying host genome input using a parallel ddPCR measurement of the diploid host gene RPP30, while Q4PCR normalizes intact proviral numbers to the cell input based on DNA equivalents after CD4 isolation and DNA extraction, as measured by DNA fluorometry (Qubit).

The third independent factor that may contribute to higher intact proviral estimates from the IPDA may be misidentification of some amplifiable sequences as intact by the PS and *env* probe combination. Sequencing results from Q4PCR provides some insights into assay performance of the PS+*env* primer/probe combination. In this large sequencing study (506 intact and 4,211 defective proviral sequences recovered), we found that the Q4PCR PS and *env* probe combination excluded 93% of defective proviruses in this data set, consistent with the original report (8). With regard to the

TABLE 3 IPDA and Q4PCR reservoir measurements of 8 representative participants[a]

Participant ID	No. of intact proviruses per 10^6 $CD4^+$ T cells		Fold difference	IPDA primer/probe 3′ mismatches (PS/*env*)	Q4PCR PS+*env* positive sequences			Sequence conservation	PS+*env* sequence no.	PS+*env* intact proviral prediction
	IPDA	Q4PCR			No. intact	No. defective	Intact (%)			
5104	233	215.28	1.1	0/0	124	34	87.9	High	High	High
5203	56	39.06	1.4	0/0	15	14	88.2	High	High	High
9254	40	27.34	1.5	0/0	42	4	91.3	High	High	High
5111	38	6.0	6.4	2/0	4	4	50.0	Low	Moderate	Moderate
UNC-346	85	12.25	6.9	0/0	8	12	40.0	High	Moderate	Moderate
UNC-432	31	1.13	27.4	2/0	1	21	4.5	Low	Moderate	Low
9246	86	1.3	66.2	0/2	1	9	10.0	Low	Moderate	Low
TSC 128	271	1.60	169.1	0/1	4	2	66.7	Moderate	Low	Moderate

[a]Increasing fold differences of the intact proviral reservoir estimates and possible contributing factors such as sequence conservation at the IPDA primer/probe binding regions, overall PCR efficiency/PS+*env* sequence numbers, and Q4PCR PS+*env* intact proviral genome prediction are depicted for each respective participant.

prediction of intact proviruses by the PS and *env* primer/probe combination, we observed that approximately 51% of the proviruses identified by the Q4PCR PS and *env* primer/probe combination are truly intact by nFGS. This is somewhat less than the 70% estimate from Bruner and colleagues based on analysis of 431 near-full-genome HIV-1 sequences (2.4%, or 10, of which were intact) obtained by single genome analysis from 28 HIV-1-infected adults (8). As observed for Q4PCR, it is also conceivable that the precision of the IPDA PS and *env* probes to identify intact proviruses varies across individuals and should be considered in the interpretation of IPDA results. However, sequencing of proviruses in IPDA PS+*env* double positive droplets is needed to confirm this potential limitation (22), as our assessment of the frequency of PS+*env*-positive proviruses that are truly intact may be limited by the efficiency of nFGS. Despite a variable ability to predict intact proviral genomes, the IPDA PS and *env* probe combination appears to measure the decay of intact proviruses, as evidenced by the differential decay of intact versus defective proviruses (15, 23). Therefore, the IPDA is a useful high-throughput assay to establish an upper limit on the frequency of provirus that may be replication-competent.

Taken together, the IPDA affords a higher throughput capacity, but the combination of PS and *env* probes can both misclassify defective sequences and fail to detect intact ones due to sequence polymorphisms. In contrast, the sequencing information in Q4PCR enables a very high specificity for intact proviruses, but it is not a high-throughput assay, and Q4PCR quantitation of sequence-confirmed intact proviruses may be limited by the inefficiency of nFGS. Both assays are subject to probe amplification failures and HIV-1 subtype variation (11, 24), though Q4PCR may be less sensitive to this because of the use of 4 probes and subsequent sequencing of positive wells. Notably, both assays require minimal cell input relative to classical QVOA, which is a clear advantage for clinical trials.

In conclusion, the differences across reservoir assays highlight that the predominantly defective and highly polymorphic proviral landscape makes the measurement of virus that is likely to cause rebound upon ART cessation extremely challenging. Nonetheless, the IPDA and Q4PCR both represent major advances in accurately quantifying and characterizing the replication-competent HIV reservoir. When used together, the two assays provide a deeper understanding of the reservoir than either assay alone and bracket true reservoir size.

MATERIALS AND METHODS

CD4 T cell isolation. Cryopreserved peripheral blood mononuclear cells (PBMCs) were viably thawed and magnetically negatively selected for CD4 T cells using either StemCell (catalog no. 17952) or Miltenyi Biotech (catalog no. 130-096-533) kits.

Intact proviral DNA assay. Detailed parameters and primer/probe sequences for the intact proviral DNA assay are as previously described (8, 25). Briefly, DNA was extracted from total CD4 T cells using the Qiagen QiaAmp DNA extraction kit as described, including the RNase A step (8). DNA was measured on the NanoDrop 1000 spectrophotometer (Thermo Fisher Scientific). Then, 12 to 16 replicate wells of up to 800 ng DNA each were combined with 2X ddPCR supermix for probes (no dUTP; Bio-Rad) and primer/probe sets for regions in PS and *env* that favor amplification of intact proviral genomes, as described (3). Final concentrations of 750 nM each primer and 250 nM each probe (6-carboxyfluorescein [FAM]/minor groove binder [MGB] for packaging signal probe; 2′-chloro-7′phenyl-1,4-dichloro-6-carboxyfluorescein [VIC]/MGB for intact *env* probe; unlabeled/MGB for hypermutated exclusionary *env* probe) were used (Thermo Fisher Scientific); all probes contained a 3′ nonfluorescent quencher. Droplets were generated on the automated droplet generator (Bio-Rad) and subsequently underwent thermocycling on the C1000 Touch thermal cycler with a 96-deep well reaction module (Bio-Rad catalog no. 1851197). Thermal cycling conditions with a 2°C ramp rate were 10 min at 95°C followed by 45 cycles (30 s at 94°C and 60 s at 59°C per cycle) and 10 min at 98°C, followed by incubation at 12°C as described (6). Droplets were read on the QX200 droplet reader (Bio-Rad catalog no. 1864003) using QuantaSoft software version 1.7.4.0917, with the exception of two samples, one (5114) with a confirmed PS polymorphism (Table S2), which made gating difficult, that were read on the QX100 droplet reader. Replicate wells were merged and analyzed in the QuantaSoft Analysis Pro software.

As described by Bruner and colleagues, a correction for DNA shearing was applied based on a separate, duplicate measurement of two regions of the diploid host gene RPP30 (4). RPP30 amplicons were spaced to match the distance between the PS and *env* IPDA HIV amplicons in order to quantify and correct for DNA shearing that occurs between the PS and *env* amplicons during the DNA extraction. DNA shearing indices were highly consistent with other reports of IPDA measurements (median, 0.35;

interquartile range [IQR], 0.33 to 0.37) (Table S2) (8, 11). The RPP30 reaction was also used to normalize for cell input as described; for each individual, a median of 1.01×10^6 (IQR, 8.35×10^5 to 1.16×10^6) CD4 T cell genome equivalents (2 copies of the RPP30 gene) were assayed (8).

Buffer-only no-template controls (NTC) as well as DNA from HIV-seronegative donors were used as a guide to set thresholds for positive droplets on each digital PCR plate. In our hands, we observed occasional low-amplitude false-positive droplets in NTC wells at a rate less than or equal to 5 copies/million CD4 T cells, depending on the run. Based on the observed false-positive rate and the subsampling constraints of digital PCR, IPDA proviral frequencies were censored at 5 copies/million CD4 T cells. In some individuals, a proviral polymorphism in primer/probe binding regions resulted in a droplet spread phenotype that was difficult to set thresholds for because of insufficient droplet separation from the negative population (Fig. 4A, Table S2). These 4 individuals were included in subsequent analyses (Table S2). In some individuals, a proviral polymorphism precluded PCR amplification of one of the IPDA amplicons (PS or *env*) (Table S2). These individuals' IPDA data were excluded from the analyses.

***gag* HIV DNA assay.** DNA was extracted from total CD4 T cells using the Qiagen QiaAmp DNA extraction kit. Up to 8 replicate wells of up to 500 ng of DNA was added to ddPCR supermix for probes (no dUTP) (Bio-Rad) with a primer/probe set overlapping the LTR-*gag* junction designed to measure group-M HIV-1 proviral load (10); 900 nM each primer and 250 nM probe were used. Droplets were generated on the automated droplet generator (Bio-Rad) and subsequently underwent thermocycling with a 2°C ramp rate for 10 min at 95°C for 45 cycles (30 s at 94°C and 60 s at 59°C per cycle) and 10 min at 98°C prior to reading on the QX200 droplet reader. RPP30 reactions were used to normalize for cell input. In 2 individuals, no positive droplets were identified. These were considered PCR amplification failures and excluded from further analysis because positive droplets were identified using the partially overlapping IPDA PS primer/probe set in the same 2 individuals.

Q4PCR. Q4PCR was performed as previously described (9). Briefly, genomic DNA from 1 million to 5 million total $CD4^+$ T cells was isolated using the Gentra Puregene cell kit (Qiagen) or phenol-chloroform, and the DNA concentration was measured using a Qubit high-sensitivity kit (Thermo Fisher Scientific). Next, an outer PCR (NFL1) was performed on genomic DNA at a single-copy dilution (previously determined by *gag* limiting dilution) using outer PCR primers BLOuterF (59-AAATCTCTA GCAGTGGCGCCCGAACAG-3′9) and BLOuterR (59-TGAGGGATCTCT AGTTACCAGAGTC-3′9 [5]). Undiluted 1-μl aliquots of the NFL1 PCR product were subjected to a Q4PCR reaction using a combination of four primer/probe sets that target conserved regions in the HIV-1 genome. Each primer/probe set consists of a forward and reverse primer pair as well as a fluorescently labeled internal hydrolysis probe as previously described (9) as follows: PS forward, 59-TCTCTCGACGCA GGACTC-3′9; reverse, 59-TCTAGCCTCCGCTAGTCAAA-3′9; probe, 59-/Cy5/TTTGGCGTA/TAO/CTCACCAGTCGCC-3′9/IAbRQSp (Integrated DNA Technologies); *env* forward, 59-AGTGGTGCAGAGAG AAAAAAGAGC-3′9; reverse, 59- GTCTGGCCTGTACCGTCAGC-3′9; probe, 59-/VIC/CCTTGGGTTC-TTGGGA-3′9/MGB (Thermo Fisher Scientific); *gag* forward, 59-ATGTTTTCAGCATTATCAGAAGGA-3′9; reverse, 59-TGCTTGATGTCCCCCCACT-3′9; probe, 59-/6-FAM/CCACCCC- AC/ZEN/AAGATTTAAACACCATGCTAA-3′9/IABkFQ (Integrated DNA Technologies); and pol forward, 59-GCA CTTTAAATTTTCCCATTAGTCCTA-3′9; reverse, 59-CAAATTTCTACTAATGCTTTTATTTTTTC-3′9; probe, 59-/NED/AAGCCAGGAATGGA-TGGCC-39/MGB (Thermo Fisher Scientific). Each Q4PCR reaction was performed in a 10-μl total reaction volume containing 5 μl TaqMan universal PCR master mix containing Rox (catalog no. 4304437; Applied Biosystems), 1 μl diluted genomic DNA, nuclease-free water, and the following primer and probe concentrations: PS, 675 nM forward and reverse primers with 187.5 nM PS internal probe; *env*, 90 nM forward and reverse primers with 25 nM *env* internal probe; gag, 337.5 nM forward and reverse primers with 93.75 nM gag internal probe; and pol, 675 nM forward and reverse primers with 187.5 nM pol internal probe. qPCR conditions were 94°C for 10 min, 40 cycles of 94°C for 15 s, and 60°C for 60 s. All qPCRs were performed in a 384-well plate format using the Applied Biosystem QuantStudio 6 Flex real-time PCR system. qPCR data analysis was performed as previously described (9). Generally, samples showing reactivity with two or more of the four qPCR probes were selected for a nested PCR (NFL2). The NFL2 reaction was performed on undiluted 1-μl aliquots of the NFL1 PCR product. Reactions were performed in a 20-μl reaction volume using Platinum *Taq* high-fidelity polymerase (Thermo Fisher Scientific) and PCR primers 275F (59-ACAGGGACCTGAAAGCGAAAG-3′9) and 280R (59-CTAGTTACC AGAGTCACACAACAGACG-3′9 [5]) at a concentration of 800 nM. Library preparation and sequencing were performed as previously described (9).

As previously described, HIV-1 sequence assembly was performed by our in-house pipeline (Defective and Intact HIV Genome Assembler), which is capable of reconstructing thousands of HIV genomes within hours via the assembly of raw sequencing reads into annotated HIV genomes (26). The steps executed by the pipeline are described briefly as follows. First, we removed PCR amplification and performed error correction using clumpify.sh from the BBtools package v38.72 (https://sourceforge.net/projects/bbmap/). A quality control check was performed with the Trim Galore package v0.6.4 (https://github.com/FelixKrueger/TrimGalore) to trim Illumina adapters and low-quality bases. We also used bbduk.sh from the BBtools package to remove possible contaminant reads using HIV genome sequences, obtained from the Los Alamos HIV database, as a positive control. We used a k-mer-based assembler, SPAdes v3.13.1, to reconstruct the HIV-1 sequences. The longest assembled contig was aligned via BLAST to a database of HIV genome sequences, obtained from Los Alamos, to set the correct orientation. Finally, the HIV genome sequence was annotated by aligning it against Hxb2 using BLAST. Sequences with double peaks, i.e., regions indicating the presence of two or more viruses in the sample (cutoff consensus identity for any residue, $<$70%), or samples with a limited number of reads (empty wells, $\leq$500 sequencing reads) were omitted from downstream analyses. In the end, sequences were classified as intact or defective (26).

Quantitative viral outgrowth assays. The quantitative and qualitative viral outgrowth assay (Q2VOA) was performed as previously described (27, 28). In brief, isolated $CD4^+$ T cells were activated with phytohemagglutinin and interleukin 2 (IL-2) (Peprotech) and cocultured with 1×10^6 irradiated PBMCs from a healthy donor in 24-well plates. After 24 h, phytohemagglutinin (PHA) was removed, and 0.1×10^6 MOLT-4/CCR5 cells were added to each well. Cultures were maintained for 2 weeks, splitting the cells 7 days after the initiation of the culture and every other day after that. Positive wells were detected by measuring p24 by enzyme-linked immunosorbent assay (ELISA). The frequency of latently infected cells was calculated through the IUPM algorithm developed by the Siliciano laboratory (http://silicianolab.johnshopkins.edu) as previously described (27).

The quantitative viral outgrowth assay (QVOA) was performed on resting CD4 T cells for participants from the UNC cohort. Lymphocytes were obtained by continuous-flow leukapheresis and isolation of resting $CD4^+$ T cells. Recovery and quantification of replication-competent virus was performed as described elsewhere (29). In general, approximately 50 million resting $CD4^+$ T cells were plated in replicate-limiting dilutions of 2.5 million (18 cultures), 0.5 million (6 cultures), or 0.1 million (6 cultures) cells per well, activated with phytohemagglutinin (Remel), a 5-fold excess of allogeneic irradiated PBMCs from a seronegative donor, and 60 U/ml interleukin 2 for 24 h. Cultures were washed and cocultivated with CD8-depleted PBMCs collected from selected HIV-seronegative donors screened for adequate CCR5 expression. Culture supernatants were harvested and assayed for virus production by p24 antigen-capture enzyme-linked immunosorbent assay (ABL). Cultures were scored positive if p24 was detected at day 15 and was increased in concentration at day 19. The number of resting $CD4^+$ T cells in infected units per billion was estimated using a maximum likelihood method (30).

Data availability. Proviral sequences have been deposited in GenBank with the accession no. MN090188 to MN090943, MT189273 to MT191207, and MW059111 to MW063110.

SUPPLEMENTAL MATERIAL

Supplemental material is available online only.

SUPPLEMENTAL FILE 1, PDF file, 0.1 MB.

ACKNOWLEDGMENTS

We thank all study participants who devoted time to our research, the Rockefeller University Hospital Research support office and nursing staff, and all members of the M.C.N. laboratory for discussions and M. Jankovic for laboratory support.

C.G. was supported by the Robert S. Wennett postdoctoral fellowship, in part by the National Center for Advancing Translational Sciences (National Institutes of Health Clinical and Translational Science Award program, grant UL1 TR001866), and by the Shapiro-Silverberg Fund for the Advancement of Translational Research. E.S. was supported by the Swiss National Science Foundation (grant number P1ZHP3_188135). This work was supported by the Bill and Melinda Gates Foundation (Collaboration for AIDS Vaccine discovery grant OPP1092074) and the National Institutes of Health (grants UM1 AI100663 and R01AI129795 to M.C.N., 1U01AI129825 to M.C., UM1AI126619 to D.M.M., R01AI134363 to N.M.A., and F30AI145588 to S.D.F.); the Einstein-Rockefeller-CUNY Center for AIDS Research (grant 1P30AI124414-01A1); BEAT-HIV Delaney (grant UM1 AI126620 to M.C.); and the Robertson Fund. M.C.N. is a Howard Hughes Medical Institute Investigator.

C.G., S.D.F., J.C.C.L., M.C., N.M.A., D.M.M., and M.C.N. designed experiments. C.G., S.D.F., E.S., J.R., R.M., J.K., K.S.J., and B.A. performed experiments. C.G., S.D.F., E.S., J.C.C.L., T.Y.O., V.R. M.C., N.M.A., D.M.M., and M.C.N. analyzed the data. C.B. and J.D.K. collected clinical data and recruited participants. C.G., S.D.F., N.M.A., R.F.S., D.M.M., and M.C.N. wrote the manuscript.

REFERENCES

1. Abdel-Mohsen M, Richman D, Siliciano RF, Nussenzweig MC, Howell BJ, Martinez-Picado J, Chomont N, Bar KJ, Yu XG, Lichterfeld M, Alcami J, Hazuda D, Bushman F, Siliciano JD, Betts MR, Spivak AM, Planelles V, Hahn BH, Smith DM, Ho YC, Buzon MJ, Gaebler C, Paiardini M, Li Q, Estes JD, Hope TJ, Kostman J, Mounzer K, Caskey M, Fox L, Frank I, Rilsey JL, Tebas P, Montaner LJ, The BEAT-HIV Delaney Collaboratory to Cure HIV-1 infection. 2020. Recommendations for measuring HIV reservoir size in cure-directed clinical trials. Nat Med 26:1339–1350. https://doi.org/10.1038/s41591-020-1022-1.
2. Falcinelli SD, Ceriani C, Margolis DM, Archin NM. 2019. New frontiers in measuring and characterizing the HIV reservoir. Front Microbiol 10:2878. https://doi.org/10.3389/fmicb.2019.02878.
3. Eriksson S, Graf EH, Dahl V, Strain MC, Yukl SA, Lysenko ES, Bosch RJ, Lai J, Chioma S, Emad F, Abdel-Mohsen M, Hoh R, Hecht F, Hunt P, Somsouk M, Wong J, Johnston R, Siliciano RF, Richman DD, O'Doherty U, Palmer S, Deeks SG, Siliciano JD. 2013. Comparative analysis of measures of viral reservoirs in HIV-1 eradication studies. PLoS Pathog 9:e1003174. https://doi.org/10.1371/journal.ppat.1003174.
4. Bruner KM, Murray AJ, Pollack RA, Soliman MG, Laskey SB, Capoferri AA, Lai J, Strain MC, Lada SM, Hoh R, Ho YC, Richman DD, Deeks SG, Siliciano JD,

Siliciano RF. 2016. Defective proviruses rapidly accumulate during acute HIV-1 infection. Nat Med 22:1043–1049. https://doi.org/10.1038/nm.4156.
5. Ho YC, Shan L, Hosmane NN, Wang J, Laskey SB, Rosenbloom DI, Lai J, Blankson JN, Siliciano JD, Siliciano RF. 2013. Replication-competent noninduced proviruses in the latent reservoir increase barrier to HIV-1 cure. Cell 155:540–551. https://doi.org/10.1016/j.cell.2013.09.020.
6. Crooks AM, Bateson R, Cope AB, Dahl NP, Griggs MK, Kuruc JD, Gay CL, Eron JJ, Margolis DM, Bosch RJ, Archin NM. 2015. Precise quantitation of the latent HIV-1 reservoir: implications for eradication strategies. J Infect Dis 212:1361–1365. https://doi.org/10.1093/infdis/jiv218.
7. Hosmane NN, Kwon KJ, Bruner KM, Capoferri AA, Beg S, Rosenbloom DI, Keele BF, Ho YC, Siliciano JD, Siliciano RF. 2017. Proliferation of latently infected CD4(+) T cells carrying replication-competent HIV-1: potential role in latent reservoir dynamics. J Exp Med 214:959–972. https://doi.org/10.1084/jem.20170193.
8. Bruner KM, Wang Z, Simonetti FR, Bender AM, Kwon KJ, Sengupta S, Fray EJ, Beg SA, Antar AAR, Jenike KM, Bertagnolli LN, Capoferri AA, Kufera JT, Timmons A, Nobles C, Gregg J, Wada N, Ho YC, Zhang H, Margolick JB, Blankson JN, Deeks SG, Bushman FD, Siliciano JD, Laird GM, Siliciano RF. 2019. A quantitative approach for measuring the reservoir of latent HIV-1 proviruses. Nature 566:120–125. https://doi.org/10.1038/s41586-019-0898-8.
9. Gaebler C, Lorenzi JCC, Oliveira TY, Nogueira L, Ramos V, Lu CL, Pai JA, Mendoza P, Jankovic M, Caskey M, Nussenzweig MC. 2019. Combination of quadruplex qPCR and next-generation sequencing for qualitative and quantitative analysis of the HIV-1 latent reservoir. J Exp Med 216:2253–2264. https://doi.org/10.1084/jem.20190896.
10. Malnati MS, Scarlatti G, Gatto F, Salvatori F, Cassina G, Rutigliano T, Volpi R, Lusso P. 2008. A universal real-time PCR assay for the quantification of group-M HIV-1 proviral load. Nat Protoc 3:1240–1248. https://doi.org/10.1038/nprot.2008.108.
11. Simonetti FR, White JA, Tumiotto C, Ritter KD, Cai M, Gandhi RT, Deeks SG, Howell BJ, Montaner LJ, Blankson JN, Martin A, Laird GM, Siliciano RF, Mellors JW, Siliciano JD. 2020. Intact proviral DNA assay analysis of large cohorts of people with HIV provides a benchmark for the frequency and composition of persistent proviral DNA. Proc Natl Acad Sci U S A 117:18692–18700. https://doi.org/10.1073/pnas.2006816117.
12. Papasavvas E, Azzoni L, Ross BN, Fair M, Yuan Z, Gyampoh K, Mackiewicz A, Sciorillo AC, Paggliuzza A, Lada SM, Wu G, Goh SL, Bahnck-Teets C, Holder DJ, Zuck PD, Damra M, Lynn KM, Tebas P, Mounzer K, Kostman JR, Abdel-Mohsen M, Richman D, Chomont N, Howell BJ, Montaner LJ. 2020. Intact HIV reservoir estimated by the intact proviral DNA assay correlates with levels of total and integrated DNA in the blood during suppressive antiretroviral therapy. Clin Infect Dis 278:1295. https://doi.org/10.1093/cid/ciaa809.
13. Kwok S, Kellogg DE, McKinney N, Spasic D, Goda L, Levenson C, Sninsky JJ. 1990. Effects of primer-template mismatches on the polymerase chain reaction: human immunodeficiency virus type 1 model studies. Nucleic Acids Res 18:999–1005. https://doi.org/10.1093/nar/18.4.999.
14. Stadhouders R, Pas SD, Anber J, Voermans J, Mes TH, Schutten M. 2010. The effect of primer-template mismatches on the detection and quantification of nucleic acids using the 5′ nuclease assay. J Mol Diagn 12:109–117. https://doi.org/10.2353/jmoldx.2010.090035.
15. Peluso MJ, Bacchetti P, Ritter KD, Beg S, Lai J, Martin JN, Hunt PW, Henrich TJ, Siliciano JD, Siliciano RF, Laird GM, Deeks SG. 2020. Differential decay of intact and defective proviral DNA in HIV-1-infected individuals on suppressive antiretroviral therapy. JCI Insight 5. https://doi.org/10.1172/jci.insight.132997.
16. Debode F, Marien A, Janssen E, Bragard C, Berben G. 2017. The influence of amplicon length on real-time PCR results. Biotechnol Agron Soc Environ 21:3–11.
17. Hiener B, Horsburgh BA, Eden JS, Barton K, Schlub TE, Lee E, von Stockenstrom S, Odevall L, Milush JM, Liegler T, Sinclair E, Hoh R, Boritz EA, Douek D, Fromentin R, Chomont N, Deeks SG, Hecht FM, Palmer S. 2017. Identification of genetically intact HIV-1 proviruses in specific CD4 (+) T cells from effectively treated participants. Cell Rep 21:813–822. https://doi.org/10.1016/j.celrep.2017.09.081.
18. Lee GQ, Orlova-Fink N, Einkauf K, Chowdhury FZ, Sun X, Harrington S, Kuo HH, Hua S, Chen HR, Ouyang Z, Reddy K, Dong K, Ndung'u T, Walker BD, Rosenberg ES, Yu XG, Lichterfeld M. 2017. Clonal expansion of genome-intact HIV-1 in functionally polarized Th1 CD4+ T cells. J Clin Invest 127:2689–2696. https://doi.org/10.1172/JCI93289.
19. Lu CL, Pai JA, Nogueira L, Mendoza P, Gruell H, Oliveira TY, Barton J, Lorenzi JCC, Cohen YZ, Cohn LB, Klein F, Caskey M, Nussenzweig MC, Jankovic M. 2018. Relationship between intact HIV-1 proviruses in circulating CD4(+) T cells and rebound viruses emerging during treatment interruption. Proc Natl Acad Sci U S A 115:E11341–E11348. https://doi.org/10.1073/pnas.1813512115.
20. Sharaf R, Lee GQ, Sun X, Etemad B, Aboukhater LM, Hu Z, Brumme ZL, Aga E, Bosch RJ, Wen Y, Namazi G, Gao C, Acosta EP, Gandhi RT, Jacobson JM, Skiest D, Margolis DM, Mitsuyasu R, Volberding P, Connick E, Kuritzkes DR, Lederman MM, Yu XG, Lichterfeld M, Li JZ. 2018. HIV-1 proviral landscapes distinguish posttreatment controllers from noncontrollers. J Clin Invest 128:4074–4085. https://doi.org/10.1172/JCI120549.
21. Vibholm LK, Lorenzi JCC, Pai JA, Cohen YZ, Oliveira TY, Barton JP, Garcia Noceda M, Lu CL, Ablanedo-Terrazas Y, Del Rio Estrada PM, Reyes-Teran G, Tolstrup M, Denton PW, Damsgaard T, Sogaard OS, Nussenzweig MC. 2019. Characterization of intact proviruses in blood and lymph node from HIV-infected individuals undergoing analytical treatment interruption. J Virol 93:1–28. https://doi.org/10.1128/JVI.01920-18.
22. Sun C, Liu L, Pérez L, Li X, Liu Y, Xu P, Boritz EA, Mullins JI, Abate AR. 2020. Droplet microfluidic sequencing of HIV genomes and integration sites. bioRxiv https://doi.org/10.1101/2020.09.25.314120:1-14.
23. Gandhi RT, Cyktor JC, Bosch RJ, Mar H, Laird GM, Martin A, Collier AC, Riddler SA, Macatangay BJ, Rinaldo CR, Eron JJ, Siliciano JD, McMahon DK, Mellors JW, Team AA. 2020. Selective decay of intact HIV-1 proviral DNA on antiretroviral therapy. J Infect Dis https://doi.org/10.1093/infdis/jiaa532.
24. Kinloch NN, Ren Y, Alberto WDC, Dong W, Khadka P, Huang SH, Mota TM, Wilson A, Shahid A, Kirkby D, Harris M, Kovacs C, Benko E, Ostrowski MA, Del Rio Estrada PM, Wimpelberg A, Cannon C, Hardy WD, MacLaren L, Goldstein H, Brumme CJ, Lee GQ, Lynch RM, Brumme ZL, Jones RB. 2020. HIV diversity considerations in the application of the intact proviral DNA assay (IPDA). bioRxiv https://doi.org/10.1101/2020.05.26.115006:1-22.
25. Falcinelli SD, Kilpatrick KW, Read J, Murtagh R, Allard B, Ghofrani S, Kirchherr J, James KS, Stuelke E, Baker C, Kuruc JD, Eron JJ, Hudgens MG, Gay CL, Margolis DM, Archin NM. 2020. Longitudinal dynamics of intact HIV proviral DNA and outgrowth virus frequencies in a cohort of ART-treated individuals. J Infect Dis https://doi.org/10.1093/infdis/jiaa718.
26. Mendoza P, Jackson JR, Oliveira TY, Gaebler C, Ramos V, Caskey M, Jankovic M, Nussenzweig MC, Cohn LB. 2020. Antigen-responsive CD4+ T cell clones contribute to the HIV-1 latent reservoir. J Exp Med 217:6441–6413. https://doi.org/10.1084/jem.20200051.
27. Lorenzi JC, Cohen YZ, Cohn LB, Kreider EF, Barton JP, Learn GH, Oliveira T, Lavine CL, Horwitz JA, Settler A, Jankovic M, Seaman MS, Chakraborty AK, Hahn BH, Caskey M, Nussenzweig MC. 2016. Paired quantitative and qualitative assessment of the replication-competent HIV-1 reservoir and comparison with integrated proviral DNA. Proc Natl Acad Sci U S A 113:E7908–E7916. https://doi.org/10.1073/pnas.1617789113.
28. Mendoza P, Gruell H, Nogueira L, Pai JA, Butler AL, Millard K, Lehmann C, Suarez I, Oliveira TY, Lorenzi JCC, Cohen YZ, Wyen C, Kummerle T, Karagounis T, Lu CL, Handl L, Unson-O'Brien C, Patel R, Ruping C, Schlotz M, Witmer-Pack M, Shimeliovich I, Kremer G, Thomas E, Seaton KE, Horowitz J, West AP, Jr, Bjorkman PJ, Tomaras GD, Gulick RM, Pfeifer N, Fatkenheuer G, Seaman MS, Klein F, Caskey M, Nussenzweig MC. 2018. Combination therapy with anti-HIV-1 antibodies maintains viral suppression. Nature 561:479–484. https://doi.org/10.1038/s41586-018-0531-2.
29. Archin NM, Vaidya NK, Kuruc JD, Liberty AL, Wiegand A, Kearney MF, Cohen MS, Coffin JM, Bosch RJ, Gay CL, Eron JJ, Margolis DM, Perelson AS. 2012. Immediate antiviral therapy appears to restrict resting CD4+ cell HIV-1 infection without accelerating the decay of latent infection. Proc Natl Acad Sci U S A 109:9523–9528. https://doi.org/10.1073/pnas.1120248109.
30. Trumble IM, Allmon AG, Archin NM, Rigdon J, Francis O, Baldoni PL, Hudgens MG. 2017. SLDAssay: a software package and Web tool for analyzing limiting dilution assays. J Immunol Methods 450:10–16. https://doi.org/10.1016/j.jim.2017.07.004.